CHAPTER IV

STRONGLY COUPLED INCOMMENSURATE SMECTIC A PHASE

4.1 INTRODUCTION

In the previous chapter we discussed the experimental results which have led to the first observation of an incommensurate smectic A phase (A_{ic}).[1,2] These studies, which were conducted on a binary system of 4-n-heptyloxyphenyl-4'-cyanobenzoyloxy benzoate (DB7OCN) and 4-n-octyloxy cyano biphenyl (8OCB), showed that the A_{ic} phase exists over a range of concentration between the A_d and A_2 phases. The X-ray diffraction pattern of this phase consists of condensed reflections at wavevectors q_o and q_o'. ($q_o = 2\pi/2\ell$, $q_o' = 2\pi/\ell'$, where ℓ is the length of the molecule and $\ell < \ell' < 2\ell$) corresponding to respectively A_2 and A_d periodicities.

The Landau phenomenological theory[3-5] discussed in the previous chapter predicts in fact two types of incommensurate phases, viz., (1) the weakly coupled incommensurate phase in which the two incommensurate density waves exist practically independent of each other and (2) the strongly coupled incommensurate phase in which the phases of the two density waves are modulated in one-dimension according to the Sine-Gordon equation.

As mentioned earlier, the X-ray diffraction pattern of the A_{ic} phase consisted of only reflections corresponding to q_o

and q_o'. Even very long exposures failed to reveal the existence of a combination reflection corresponding to the sum or difference of the wavevectors. It can therefore be surmised that A_{ic} is of the weakly coupled type.

Recently Fontes et al.[6] have observed in a monolayer (A_1) phase (with a condensed diffraction peak at $2q_o$) the existence of two diffuse scattering peaks: one centred at q_o', an incommensurate wavevector, and the other at $q_s = 2q_o - q_o'$. These results indicated the presence of strong incommensurate fluctuations in the A_1 phase. But on cooling the A_1 phase, the diffuse sctttering profile evolved into an off-axis pattern characteristic of an antiphase and thus the strongly coupled incommensurate A phase remained elusive.

We have undertaken studies on a binary system of 4-n-octyloxyphenyl-4'-cyanobenzoyloxy benzoate (DB8OCN) and 4-n-octyloxybenzoyloxy-4"-cyanoazobenzene (8OBCAB). These studies which have led to the first observation of the strongly coupled incommensurate phase are described in this chapter.

4.2 MATERIALS

The molecular structures of the compounds 4-n-octyloxyphenyl-4'-cyanobenzoyloxy benzoate (DB8OCN) and 4-n-octyloxy-4"-benzoyloxy-cyanoazobenzene (8OBCAB) are shown in Fig. 4.1. The transition

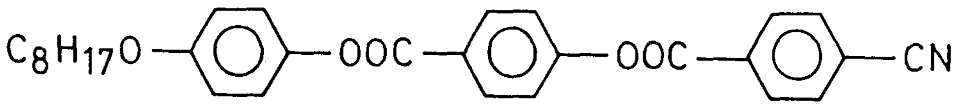

$K \xrightarrow{127\,°C} Ad \xrightarrow{197.4\,°C} N \xrightarrow{241\,°C} I$

4-n-octy loxy phenyl-4'-cyanobenzoy loxy benzoate (DB8O.CN)

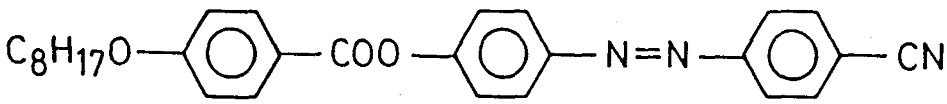

$K \xrightarrow{93\,°C} A_1 \xrightarrow{100.3\,°C} N \xrightarrow{257\ 5\,°C} I$

4-n-octyloxy benzoyloxy-4'-cyanoazobenzene (8OBCAB)

***Fiquze** 4.1*

The** molecular formulae of DB8OCN **and** 8OBCAB **along with
***theiz** phase transition temperatures.*

temperatures of these two compounds are also given in the same figure.

4.3 EXPERIMENTAL

The X-ray diffraction experiments were carried out using a computer controlled Guinier diffractometer (Huber 644). The sample was taken in a 0.5 mm diameter Lindemann glass capillary whose ends were then sealed. To obtain a monodomain sample, the sample was cooled very slowly from the nematic phase in the presence of a 2.4 T magnetic field. A detailed description of the experimental set up has already been given in Chapter II. The precision in the determination of the wavevector at any temperature was 2×10^{-4} Å^{-1} while the temperature was maintained constant to ± 10 mK during any measurement. All the scans were taken along the equatorial ($q_{\perp} = 0$) direction. The longitudinal resolution ($\Delta q_{||}$) was about 1×10^{-3} Å^{-1}.

4.4 RESULTS AND DISCUSSION

The partial phase diagram of the DB8OCN - 8OBCAB binary system is shown in Fig. 4.2. Interestingly the compounds have nearly the <u>same molecular length</u> (~ 32 Å). This phase diagram, which has been obtained on the basis of optical microscopic, X-ray and differential scanning calorimetry studies, is extremely rich - there are three types of incommensurate A phases in addition to the reentrant nematic (N_{re}), A_d, A_1 and A_2 phases. We shall first

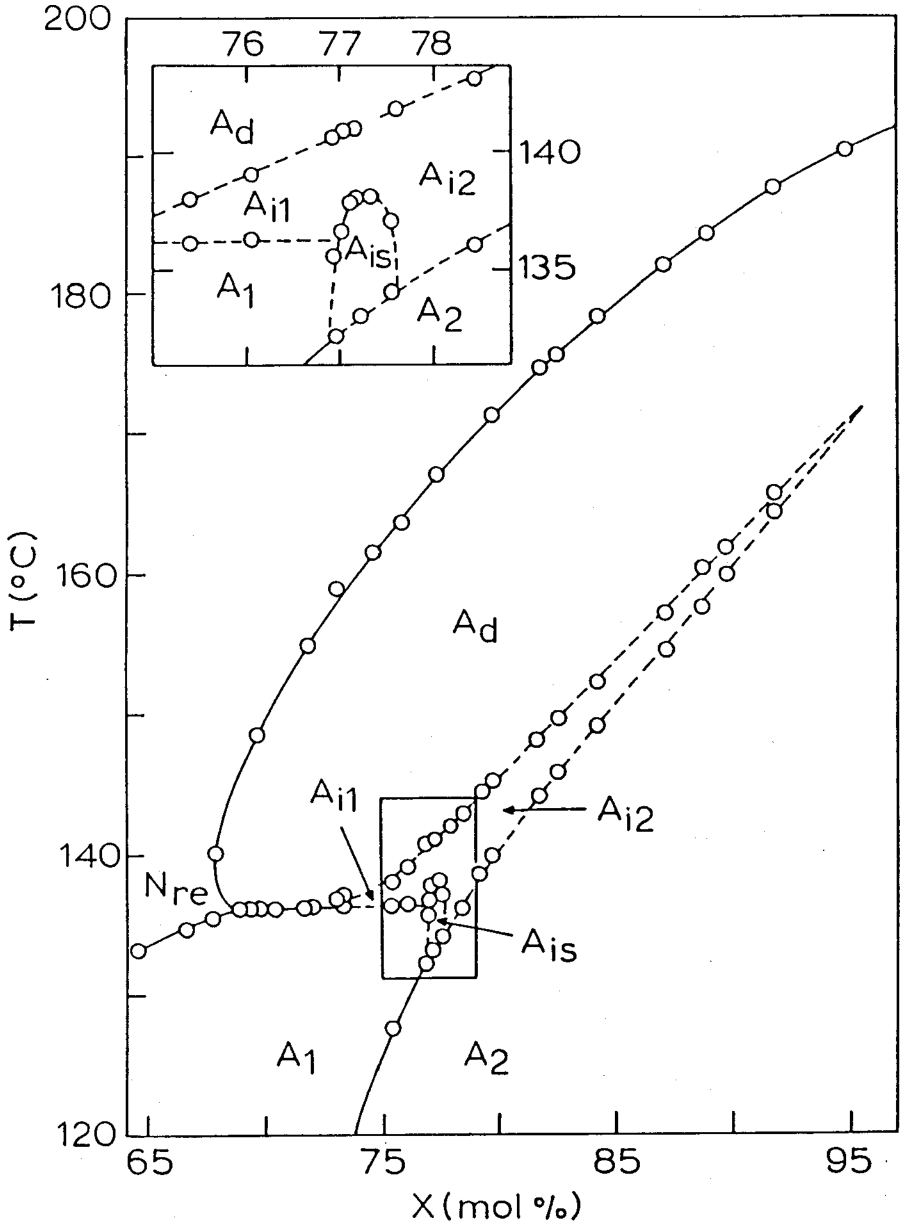

Figure 4.2

Partial temperature concentration diagram for the binary mixtures of DB8OCN in 8OBCAB. X is the mol % of DB8OCN in the mixture. A_{i1} and A_{i2} are weakly coupled incommensurate phases, while A_{is} is the strongly coupled incommensurate phase. The inset shows the region of the T-X diagram in the vicinity of the A_{ic} phase on an enlarged scale. The dashed lines mark the domain of existence o6 the incommensurate phase.

summarize the main features of this diagram and then present the results of our X-ray studies which identify the different A phases:

(1) Starting from the DB8OCN side, for $X > 95$ (where X is the mol per cent of DB8OCN in the mixture) there is a continuous evolution of A_2 from A_d, similar to the behaviour of DB7OCN seen earlier.[7]

(ii) For $72 < X < 95$ the weakly coupled incommensurate phase exists. Over a major portion of the phase diagram, it exists between A_d and A_2 phases while over a smaller region (on the lower X side) it intervenes between A_d and A_1 phases. They have been designated as A_{i2} and A_{i1} respectively.

(iii) For $69 < X < 72$, a direct $A_d - A_1$ transition is observed which ends at the $A_1 - N_{re} - A_d$ point on the lower X side.

iv) Over a very narrow region of X, viz., $76.9 < X < 77.6$, the strongly coupled incommensurate phase (designated as A_{is}) occurs. The region of the phase diagram surrounding A_{is} is shown on the enlarged scale in the inset of Fig. 4.2.

We shall now discuss the results of our X-ray diffraction experiments which have helped us to unambiguously characterize the different phases marked in the phase diagram. We have studied a large number of concentrations covering the entire range of phase diagram shown in Fig. 4.2, but data for only a few representative concentrations characterising the different regions of the phase diagram are presented here. In the case of $X = 95.5$ mixture, the wavevector variation with temperature is shown in Fig. 4.3. It is seen that the wavevector q_o' continuously evolves into q_o, i.e., the A_d phase goes over to the A_2 phase without a phase transition. This is very similar to the results on DB7OCN.[7] For X = 81.8 mixture the wavevector variation with temperature is shown in Fig. 4.4. It is seen that in the A_d phase q_o' shows a decrease with decrease in temperature. The onset of the A_{i2} phase is signalled by the appearance of condensed peaks at q_o and at the second harmonic $2q_o$. At the same temperature, q_o' reverses its trend. The variation of q_o' with temperature in the A_{i2} phase is opposite to that in the A_d phase. On transforming to the A_2 phase, q_o' disappears. The wavevector variations (q_o' and q_o) with temperature are similar to that observed earlier in the DB7OCN/8OCB binary system described in Chapter III. (We have earlier referred to the A_{i2} phase as A_{ic}). For the X = 74.8 mixture the wavevector variation is shown in Fig. 4.5. For this mixture the sequence of transitions on cooling is $A_d \rightarrow A_{i1} \rightarrow A$. The wavevector variation in the A_d phase is very similar to that observed for the X = 81.8 mixture, i.e., q'_o shows a steep decrease with decrease in temperature. In the case of the incommensurate (A_{i1}) phase the wavevector characterizing this phase are q_o' and $2q_o$. Interestingly, the variation of q_o' in the A_{i1} phase is similar to the variation of q'_o in the A_{i2} case. An additional feature of the results for the X = 74.8 mixture (Fig. 4.5) is the observtion of a diffuse scatte-

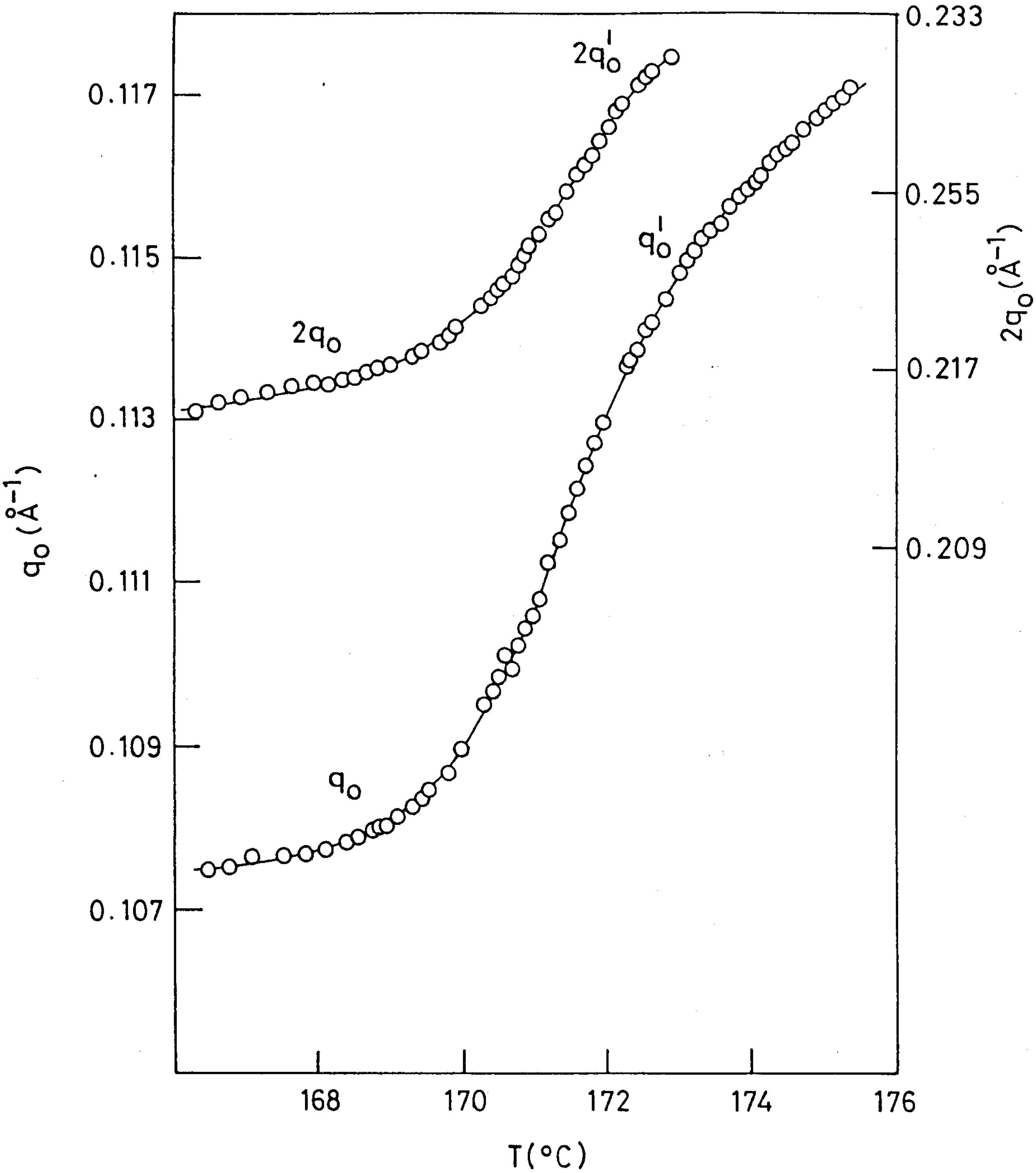

Figure 4.3

Temperature variation of the wavevectors for X = 95.5 mol % mixture. A_d phase continuously evolves into A_2 phase.

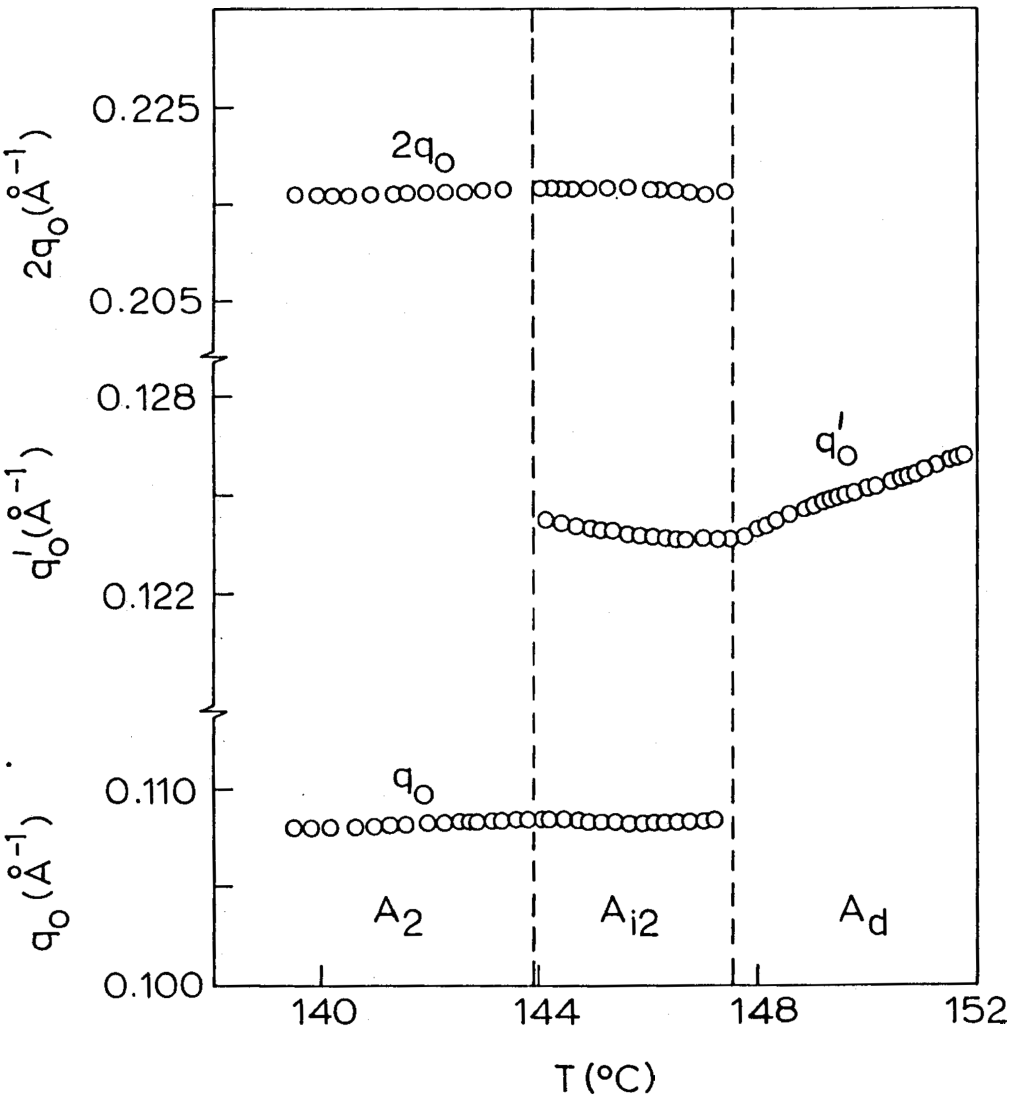

Figure 4.4

Tempezature variation of the wavevectozo in the A_d, A_{i2} and A_2 phases for X = 81.8 mixture. AN the data cozzeopond to condenoed peaks.

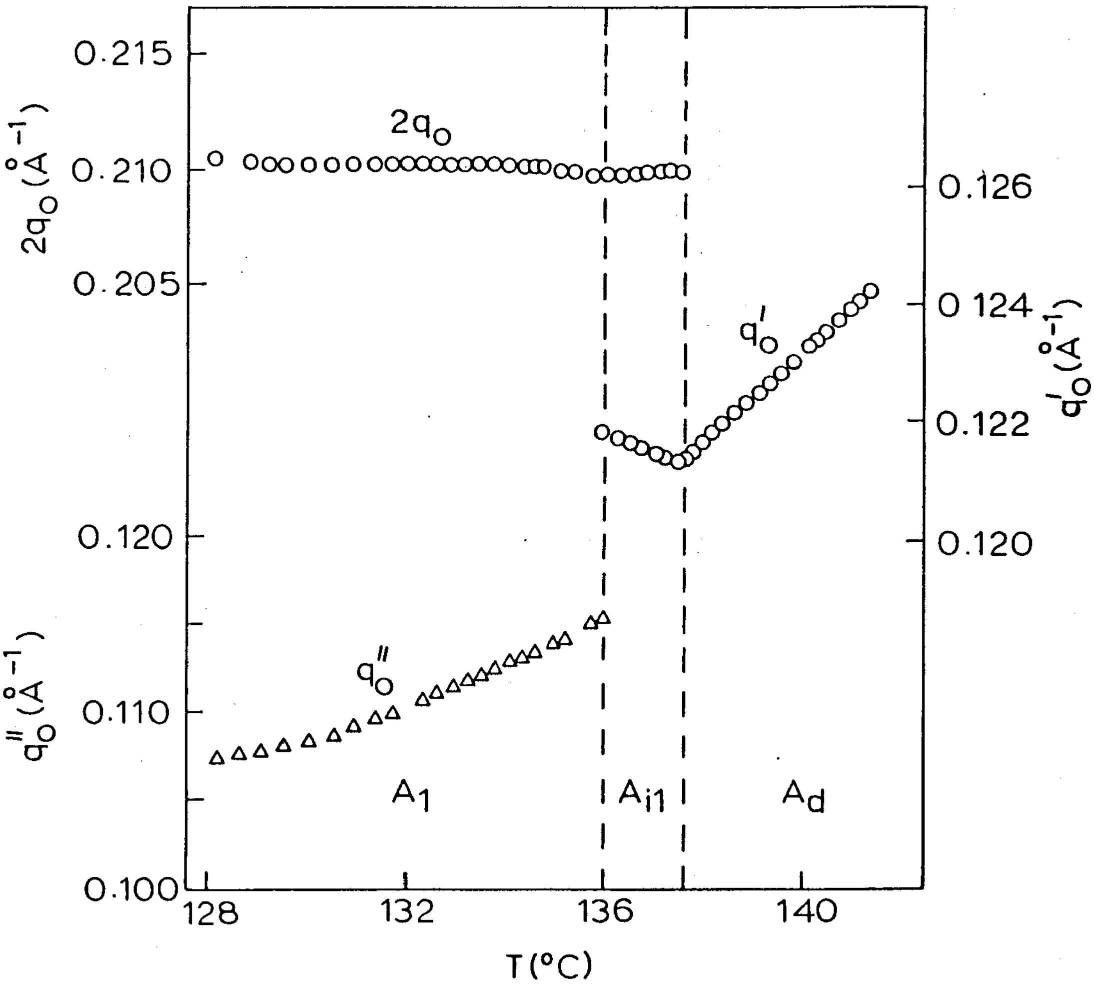

Figure 4.5

Temperature variation of the wavevectors in the A_d, A_{i1} and A_1 phases for X = 14.6 mixture. Circles indicate that the diffraction peaks are condensed while triangles indicate diffuse maxima.

ring peak centred around another incommensurate wavevector q_o'' ($\neq q_o'$). With decrease of temperature the q_o'' value was found to be decreasing and finally at the transition to the A_2 phase (not shown in the figure) the diffuse modulation condenses at a wavevector q_o corresponding to the A_2 phase. A particular feature of the A_2 phase is that the intensity of the peak at $2q_o$ is found to be three times larger than that at q_o. Although this is in agreement with the relative intensities predicted theoretically,[8] it is opposite to what has been generally seen in the A_2 phase (see e.g., Ref. 9). It should also be mentioned that no combination reflections were observed in either A_{i2} or A_{i1} phases showing thereby that both these are weakly coupled incommensurate phases.

The data for the $X = 77.3$ mixture is shown in Fig. 4.6. This figure shows many important fetures. On cooling from the A_d phase q_o' decreases with decrease in temperature. On further cooling the A_d phase goes over to the A_{i2} phase (with modulations at q_o', q_o and $2q_o$) and then to the A_{i1} phase which has, in addition to the peaks at q_o' and $2q_o$, a diffuse modulation at q_o''. The X-ray diffraction pattern in this phase is similar to that observed in the same phase of the $X = 74.8$ mixture. As the temperature is decreased further, diffuse q_o'' condenses at a temperature of 138.6°C and, simultaneously, another peak appears at q_s, while the third peak at $2q_o$ continues unaffected. This signifies the onset of the A_{is} phase with three condensed diffraction peaks. The schematic

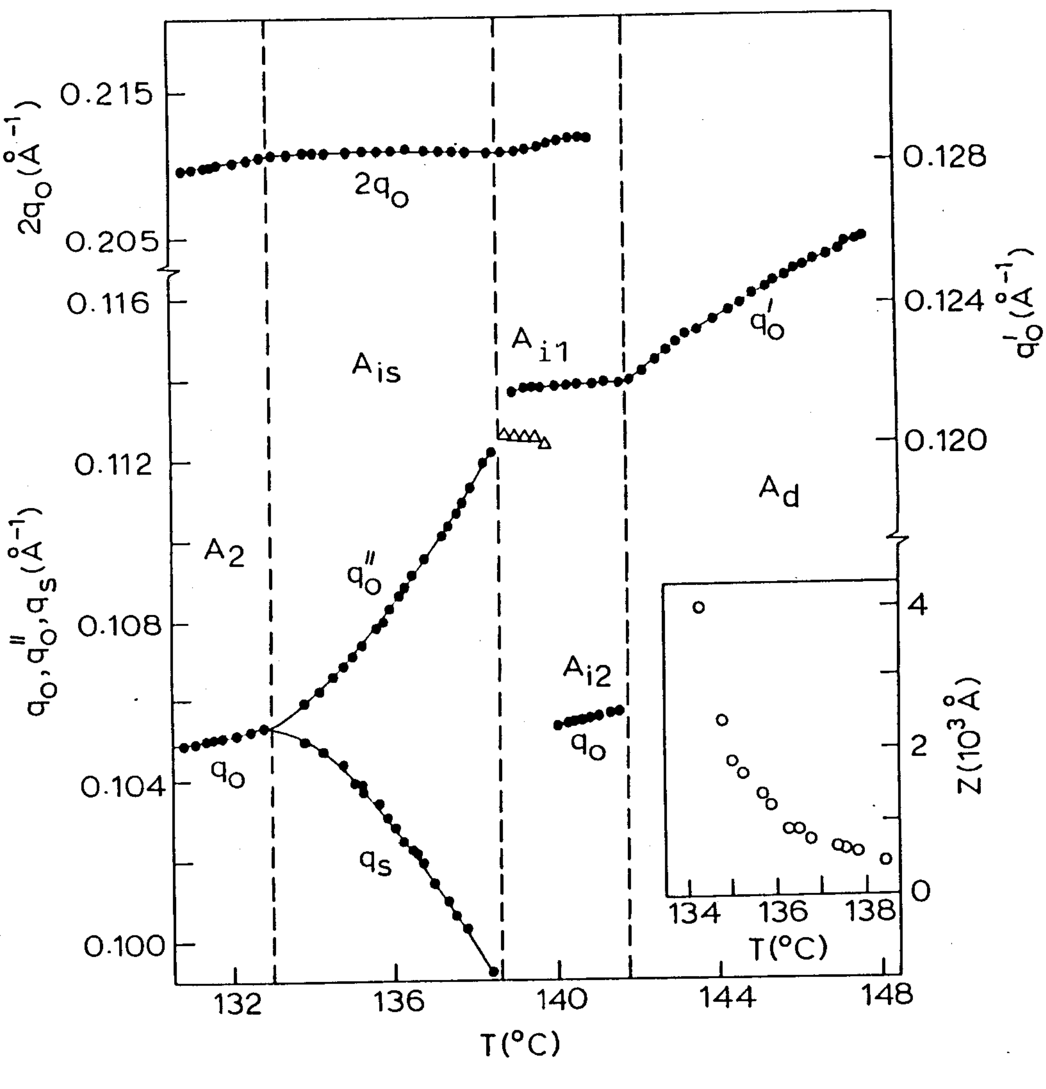

Figure 4.6

Temperature variation of the wavevectors in the different phases for X = 77.3 mixtuie. Filled circles signify that the diffraction peaks are condensed while the open triangles denote diffuse maxima. In the strongly coupled incommesurate A_{is} phase a satellite reflection is seen at $q_s = 2q_0 - q''_0$, showing the existence of solitons. The inset shows the divergence of the soliton peziodicity (Z) as the commensurate A_2 phase is appzoached.

representation of the X-ray diffraction patterns in the different A phases for the X = 77.3 mixture is shown in Fig. 4.7. Typical diffractometer scans showing the three peaks at $2q_o$, q''_o and q_s are reproduced in Fig.4.8. It is clearly seen that all of them are <u>condensed</u> peaks, the intensity of q_s being comparable to that of q''_o. We also ascertained by taking X-ray photographs that the three modulations are indeed collinear and that the in-plane order is liquid-like. The value of q_s was found to be, within the experimental uncertainties, exactly equal to $2q_o - q''_o$. The actual data (at different temperatures) of $2q_0$ and q''_0 and q_s are given in the Table 4.1 along with the q_s value obtained by the arithmetic calculation of $2q_o - q''_o$. It is clear from the table that at all temperatures in the A_{is} phase, q_s is indeed equal to $2q_o - q''_o$ showing thereby that q_s is a satellite reflection. This in turn implies that <u>the incommensurate modulations are strongly coupled</u>. Thus we have observed a strongly coupled incommensurte A phase.

We shall now consider the temperature variation of q_s and q''_o in the A_{is} phase (see Fig. 4.6). As the temperature is decreased, these wavevectors converge towards their mean value until finally they 'lock-in' at the commensurate wavevector q_o. Thus the $A_{is} - A_2$ transition is a typical <u>incommensurate - commensurate transition</u>. The existence of the satellite reflection at a wavevector q_s which is collinear with q''_o and $2q_o$ clerly indicates that the incommensurate density waves are modulated in 1-dimension. The structure

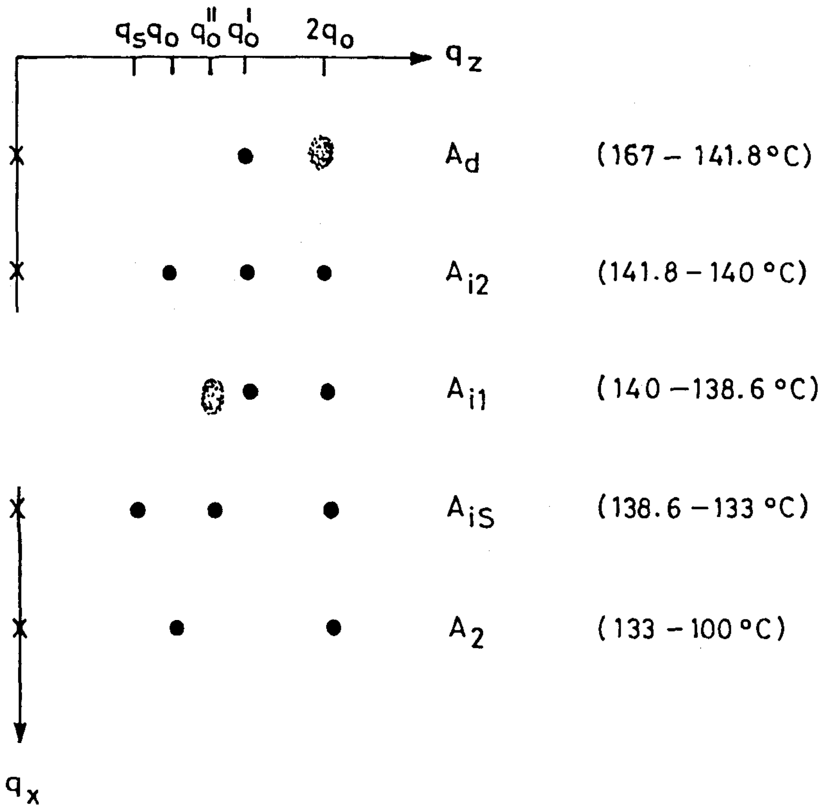

Figure 4.7

Schematic representation of the characteristic Xray diffraction patterns in the different A phases of X = 77.3 mixture. Here X stands for the direct beam, • denotes a condensed peak and ❂ *refers to a diffuse maximum. The corresponding wavevectors are marked on the q_z line. Note that all the diffraction spots are along the q_z direction, i.e., they are collinear. The temperature range of the phase is given within brackets in each case.*

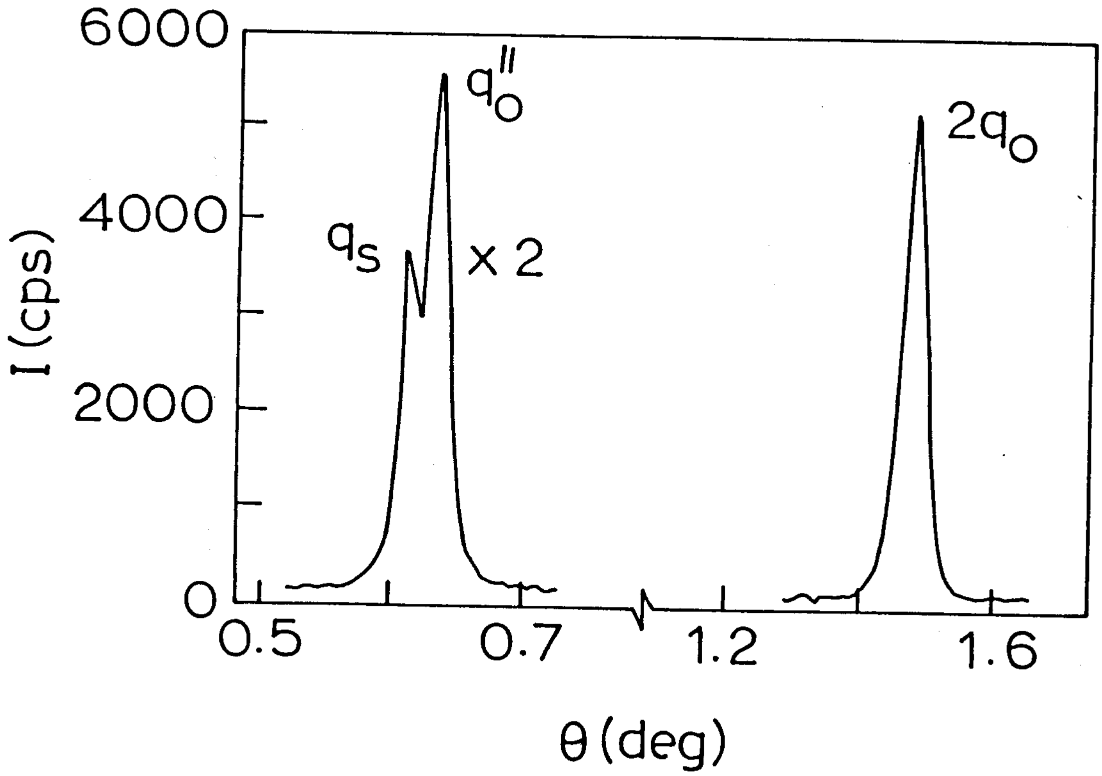

Figure 4.8

Typical diffractometer scans taken along the equatorial ($q_{\perp} = 0$) direction in the A_{is} phase for $X = 77.3$ mixture showing the X-ray scattered intensity I (counts per second) as a function of the scattering angle (θ). The wavevectors corresponding these condensed peaks have been marked. The intensities of q_s and $q_0^{\parallel}$ have been multipled by a factor of 2.

Table 4.1

Experimentally determined values of the wavevectors $2q_0$, q''_0 and q_s at different temperatures in the A_{is} phase (the value of q_s obtained calculation is also given).

Temperature	$2q_0$	q''_0	q_s (exptl.)	q_s(calc.) $= 2q_0 - q''$
136.90	0.2110	0.1121	0.0982	0.0989
137.27	0.2112	0.1109	0.1002	0.1002
136.97	0.2110	0.1103	0.1006	0.1007
136.81	0.2112	0.1104	0.1009	0.1008
136.20	0.2112	0.1095	0.1014	0.1017
135.97	0.2112	0.1088	0.1018	0.1024
135.73	0.2109	0.1086	0.1017	0.1023
135.18	0.2109	0.1079	0.1034	0.1030
135.36	0.2109	0.1081	0.1030	0.1028
134.70	0.2110	0.1076	0.1036	0.1034
134.74	0.2109	0.1075	0.1038	0.1033
134.50	0.2109	0.1073	0.1038	0.1036
134.25	0.2109	0.1070	0.1043	0.1039
133.77	0.2109	0.1063	0.1047	0.1046

of A_{is} can therefore be considered as a periodic array of solitons or an array of domain walls in one-dimension (i.e., along the director). As the temperature is decreased towards the A_2 phase, the periodicity of the solitons, which is given by $Z = 2\pi/(q_o'' - q_s)$, diverges (see inset of Fig. 4.6) as predicted by theory.[10]

Finally, it is relevant to comment on a theoretical phase diagram which has been evaluated on the basis of the phenomenological model. The theory predicts a tetracritical point at which the incommensurate A phase joins the intersection of the $A_1 - N$ and $N - A_d$ boundaries. The theory also envisages the alternative possibility that the domain of the incommensurate phase may be disconnected from the nematic phase by an $A_d - A_1$ phase boundary. The latter picture is in qualitative agreement with the experimental phase diagram shown in Fig. 4.2. However, while no distinction is made between the strongly and weakly coupled incommensurate phases in the theoretical phase diagram, the experimental results show that the domain of stability of the former is much smaller than that of the latter. It is also remarkable that a binary system whose constituent compounds have nearly the same molecular length produces such a rich variety of A phases. This shows that the polymorphism of smectic A should be very delicately dependent on the nature of the molecular interactions.

REFERENCES

1 B.R.Ratna, R.Shashidhar and V.N.Raja, Phys. Rev. Lett., 55, 1476 (1985)

2 B.R.Ratna, R.Shashidhar and V.N.Raja, in "Incommensurate in Crystals, Liquid Crystals, and Quasi Crystls", Eds. J.F.Scott and N.A.Clark (Plenum, New York, 1987), p. 259.

3 J. Prost, in "Liquid Crystals of One- and Two-Dimensional Order', Eds. W.Helfrich and G.Heppke (Springer-Verlag, Berlin, 1980), p. 125.

4 J. Prost and P. Barois, J. Chim. Phys. Chim.Biol., 80, 65 (1983)

5 P.Barois, J. Pommier and J. Prost, in "Solitons in Liquid Crysals", Eds. Lui Lam and J. Prost (to be published)

6 E.Fontes, P.A.Heiney, P.Barois and A.M.Levelut, Phys. Rev. Lett., 60, 1138 (1988)

7 S.Krishna Prasad, R.Shashidhar, B.R.Ratna, B.K. Sadashiva, G.Heppke and S.Pfeiffer, Liquid Cryst., 2, 111 (1987)

8 P.Barois, J. Prost and T.C.Lubensky, J. de Phys., 46, 391 (1985)

9 R.Shashidhar, B.R.Ratna, S.Krishna Prasad, S.Somasekhara and G.Heppke, Phys. Rev. Lett., 59, 1209 (1987)

10 P. Barois, "Problems d'incommensurabiliti dans les cristaux liquides i polaires: smectiques frustre's", These de specialite Universitide Bordeaux l, 1981, No. 1748.